Hindawi
International Journal of Polymer Science
Volume 2019, Article ID 8053808, 11 pages
https://doi.org/10.1155/2019/8053808

Research Article

Using Externally Bonded CFRP to Repair a PCCP with Broken Wires under Combined Loads

Kejie Zhai,[1] Hongyuan Fang,[2,3,4] Bing Fu,[5] Fuming Wang,[1,2,3,4] and Benyue Hu[2,3,4]

[1]*School of Civil Engineering, Sun Yat-sen University, Guangzhou 510275, China*
[2]*College of Water Conservancy & Environmental Engineering, Zhengzhou University, Zhengzhou 450001, China*
[3]*National Local Joint Engineering Laboratory of Major Infrastructure Testing and Rehabilitation Technology, Zhengzhou 450001, China*
[4]*Collaborative Innovation Center of Water Conservancy and Transportation Infrastructure Safety, Henan Province, Zhengzhou 450001, China*
[5]*School of Civil and Transportation Engineering, Guangdong University of Technology, Guangzhou 510006, China*

Correspondence should be addressed to Hongyuan Fang; 18337192244@163.com

Received 29 March 2019; Revised 5 September 2019; Accepted 11 September 2019; Published 20 October 2019

Academic Editor: Gianluca Cicala

Prestressed concrete cylinder pipe (PCCP) is widely used for long-distance water pipelines throughout the world. However, prestressing wire breakage is the most common form of PCCP damage. For some pipelines that cannot be shut down, a new technique for in-service PCCP repair by externally bonding the pipe with layers of carbon fiber reinforced polymer (CFRP) was proposed. A set of three-dimensional finite element models of the repaired PCCP have been proposed and implemented in the ABAQUS software, which took into account the soil pressure, the weight of the PCCP, the weight of the water, and the hydrostatic pressure. The stress–strain features of the PCCP repaired with CFRP of various thicknesses were analyzed. The stress–strain features of different wire breakage rates for the repaired PCCP were also analyzed. The results showed that the strains and stresses decreased at the springline if the PCCP was repaired with CFRP, which improved the operation of the PCCP. It has been found that the wire breakage rates had a significant effect on the strains and stresses of each PCCP component, but CFRP failed to reach its potential tensile strength when other materials were broken.

1. Introduction

The first prestressed concrete cylinder pipe (PCCP) was designed and manufactured in 1939. PCCP is widely used in water transfer projects all over the world because it resists external pressures and internal forces and it is impermeable. PCCP is a composite structure consisting of a concrete pipe core encased in a steel cylinder surrounded by prestressing wires and a mortar coating. Structurally, PCCP can be divided into embedded cylinder (ECP) and lined cylinder (LCP) types [1, 2].

PCCP is subjected to different loads from external pressures and internal forces during its service life. Many studies have focused on PCCP loading. Ross [3] analyzed the strain responses of various structural materials by crushing and bending tests with the pipe under hydrostatic pressure. Kennison [4] and McCall [5] examined the behaviour of PCCPs in response to combined loads using internal and external load tests. Gomez and Munoz [6] used two- and three- dimensional finite element models to investigate the effects of gradual loss of tension in the prestressing wires. Zhang et al. [7] used ANSYS to examine the mechanical properties of the PCCP during manufacture, construction, and operation, and they developed models for PCCP design, manufacture and operation. Dou et al. [8, 9] tested the various PCCP layers during pressurization using Brillouin optical time-domain analysis (BOTDA) and fiber Bragg grating (FBG) sensing techniques. Zhang et al. [10] comprehensively tested a jacking prestressed concrete cylinder pipe (JPCCP) with external loads, internal hydrostatic pressure, and combined loads and described the failure of the JPCCP under combined loads.

Zarghamee et al. [11, 12] studied the separation of mortar and concrete under different mortar–prestressing wire bonding conditions through tests and finite element analysis. Hu et al. [13] conducted an external load prototype test and modeled the PCCP used in the South-to-North Water Diversion Project to predict the effects of existing cracks in the concrete core of the PCCP. Gong et al. [14] conducted full-scale experimental research and modeling to evaluate the damage caused during pipe jacking by different jacking forces and different geological conditions. Sun et al. [15] combined testing and numerical analysis to identify the key factors controlling the rotation of PCCP pipelines and to guide PCCP design and engineering on soft soil foundations. Zhang et al. [16] conducted a full-scale test on a new JPCCP to determine changes in pipe–soil contact stress during jacking and to provide a better basis for the manufacture and construction of the JPCCP. Xu et al. [17] used BOTDA to evaluate mortar cracks and PCCP structural states.

PCCP performance deteriorates as the pipe ages. The pipe corrodes easily in the complex underground environment, and the prestressing wires may break, which reduces the integrity of the pipeline. There have been studies of PCCPs with broken wires. Diab and Bonierbale [18] created two-dimensional and three-dimensional finite element models and developed effective repair procedures. Zarghamee et al. [19–21] studied the characteristics of broken PCCPs with different diameters under combined loads using nonlinear finite element models. They empirically tested the failure modes and ultimate bearing capacity of a PCCP with broken prestressing wires to give probabilistic risk assessments for a PCCP with broken wires. Hu and Shen [22] used finite nonlinear element analysis with empirical testing and found that when the number of broken wires reaches a certain value, the concrete core is more likely to crack, which affects the long-term operation of a PCCP. Ge and Sinha [23] developed a theoretical method for calculating the length of prestress loss. They suggested that broken wires do not have a significant impact on a PCCP with good mortar adhesion. Hajali et al. [24–26] considered the pipe–soil interaction, the interaction between neighboring pipes, and internal and external loads in modeling the effects of the position and number of broken wires on a PCCP using a three-dimensional finite element model.

The breakage of prestressing wires can easily cause a pipe burst event, resulting in almost incalculable loss. Reinforcement and repair of the PCCP has received increased attention. Carbon fiber reinforced polymer (CFRP) is widely used as reinforcement because of its light weight, high strength, corrosion resistance, and many other advantages [27–30]. CFRP liner installation has gradually become the focus of scholarly research. Lee and Karbhari [31] studied the mechanical behavior of CFRP lining under external and internal forces by testing PCCP cross-sections. Engindeniz et al. [32, 33] developed quality assurance procedures and testing standards to be followed before, during and after the use of CFRP liner to repair a PCCP. Then, the effects on the design, materials, installation and quality control regulations of the AWWA were identified through testing. Alkhrdaji [34] introduced a hybrid FRP liner repair technology and verified its reliability through testing. Lee and Lee [35] used finite element analysis to examine the effects of the number of CFRP liners, the lining angle, and the number of broken wires on a PCCP. Hu et al. [36] modeled the complex CFRP–concrete bond interface using ABAQUS software for finite element analysis and analyzed the CFRP liner in repairing a PCCP under combined loads.

The preceding results show that PCCP can be effectively repaired. However, the use of CFRP liner in repairs requires the pipe flow to be interrupted over a long construction period. It is also difficult to use CFRP liner to repair small diameter PCCP. A method of repairing a PCCP with externally bonded CFRP was proposed. We used ABAQUS finite element software to create a three-dimensional model for the repair of a PCCP with broken wires using externally bonded CFRP layers. The 3D FEM model takes account of the pressure of the soil, the weight of the PCCP, the weight of the water, and the hydrostatic pressure. We analyzed the effect of using CFRP externally to repair a PCCP with broken wires under combined loads and the effect of the number of CFRP layers and the proportion of broken wires on the repair. The research undertaken in this study provides novel ideas and methods for PCCP reinforcement, and the results can guide PCCP repair in practice.

2. 3D FEM Model Description

2.1. Model State Description. The type of PCCP used in the 3D FEM model is ECP. The structure of ECP is shown in Figure 1. The geometry of PCCP is shown in Table 1.

Concrete and mortar were modeled using three-dimensional eight-node solid brick elements to represent them [37]. The concrete and mortar were meshed as 25200 and 5459 elements. Two failure mechanisms were associated with them in the 3D FEM model: compressive crushing and tensile cracking. The ABAQUS concrete damaged plasticity model (CDP) was used to describe the mechanical behavior of the concrete and mortar, which were both classified as brittle materials. The concrete damaged plasticity model is shown in Figure 2.

In Figure 2, σ_c is the compressive stress of the concrete; σ_t is the tensile stress of the concrete; σ_{c0} is the maximum elastic compression stress; σ_{t0} is the maximum elastic tensile stress; σ_{cu} is the maximum compression stress; d_c is the damage factor of compression; d_t is the damage factor of tension; ω_c is the compressive recovery factor; ω_t is the tensile recovery factor; E_0 is the initial elastic modulus.

The steel cylinder was represented by a four-node quadrilateral element with reduced integration (S4R) because it is classified as a thin-walled structure. The steel cylinder was meshed as 1380 elements.

The wrapping stress of the prestressing wires is 70% of the tensile strength of the wire. The stress–strain relation of the prestressing wire is shown in Equation (1).

$$f_s = \begin{cases} \varepsilon_s E_s & \varepsilon_s \le f_{sg}/E_s \\ f_{su}\left\{1 - \left[1 - 0.6133(\varepsilon_s E_s / f_{su})\right]^{2.25}\right\} & \varepsilon_s > f_{sg}/E_s \end{cases} \quad (1)$$

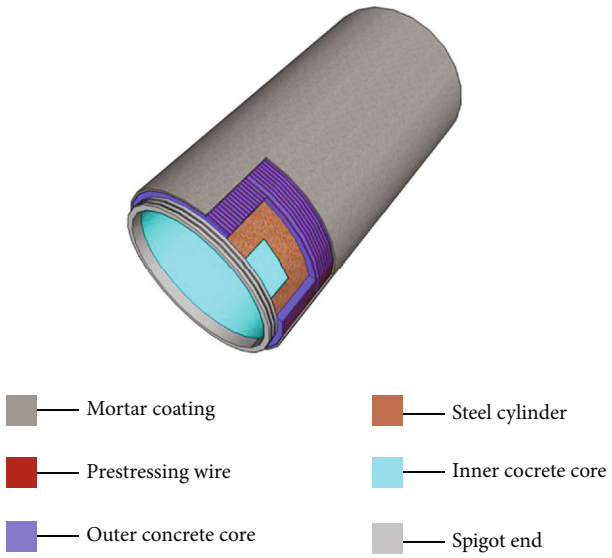

Figure 1: Structure of ECP.

Table 1: Geometry of PCCP.

Dimension	Size (mm)
Length of PCCP (h)	6000
Inner diameter of PCCP (D_i)	2800
Total concrete thickness including cylinder (h_c)	200
Thickness of the steel cylinder (t_y)	1.5
Diameter of steel cylinder (D_y)	2923
Diameter of wires (d)	7
Spacing of wires	14.1
Thickness of mortar (t_m)	32

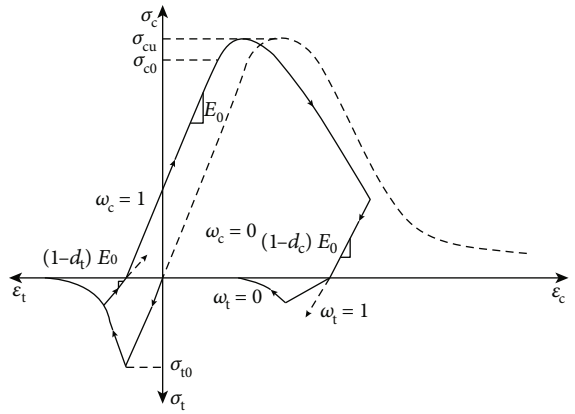

Figure 2: ABAQUS concrete damaged plasticity model.

where: f_s is the stress of the prestressing wire; ε_s is the strain of the prestressing wire; E_s is the elastic modulus of the prestressing wire; f_{su} is the tensile strength of the prestressing wire; and $f_{sg} = 0.75 \times f_{su}$.

A three-dimensional truss element (T3D2) was used to represent the prestressing wires. The prestressing wires were considered as many rings, and every ring was meshed as 80 elements.

Three methods can be used for prestressing wires: equivalent load, cooling, and wrapping [38]. We used the cooling method. The cooling value is determined by:

$$\Delta t = \frac{F}{\alpha E A} \tag{2}$$

where: Δt is the temperature decrease (°C); F is the stress of the prestressing wire (N); α is the coefficient of expansion of the prestressing wire (10^{-6}/°C); E is the elastic modulus of the prestressing wire (Pa); and A is the cross-sectional area of the prestressing wire (m^2).

In the model, all broken wires were removed and the position of the broken wires is the midpoint of the PCCP.

The soil was represented as three-dimensional eight-node brick elements described by the Mohr–Coulomb model. The depth of soil covering the PCCP was 5 m, and there was soil cushion under the pipe.

The CFRP was represented as a four-node quadrilateral element with reduced integration (S4R), like the steel cylinder, and it was classified as elastic-brittle material. The direction of the material is shown in Figure 3(c). Each layer of CFRP is 0.167 mm thick and 500 mm wide.

2.2. Material Properties and the Model of Contact. The mechanical properties of the materials used in the model are shown in Table 2.

Pipe–soil and CFRP–soil contact was simulated using the surface-to-surface contact technique. This is described as "hard contact" with a penalty condition to allow the stress transmission between the surfaces. The concrete and mortar were combined, as were the CFRP and the mortar. The prestressing wires and the steel cylinder were embedded in the concrete core. The bottom surface of the soil was fully constrained, the normal directions were assigned to the shell, and the top surface was not constrained [39, 40].

2.3. Model Verification of PCCP. The size and material parameters of the PCCP model used in this paper are the same as those in [41]. Also, the calculation results of the soilless PCCP model were compared with that in reference [41], as shown in Figure 4. The initial strain was calculated from the beginning of internal pressure. Figure 4 shows that the PCCP model agrees well with the results of reference, which verifies the reliability of the PCCP structural model.

3. Effects of Different CFRP Thicknesses on the Repair

Externally bonded CFRPs with different thicknesses were modeled to study the effects of repair when there were combined loads. The proportion of broken wires on the PCCP was 10%. The five models had identical conditions except for the thickness of the CFRP. The five different models are shown in Table 3.

Using a hydrostatic pressure of 1.12 MPa, which is the designed value, the effects of the repair on the whole pipe

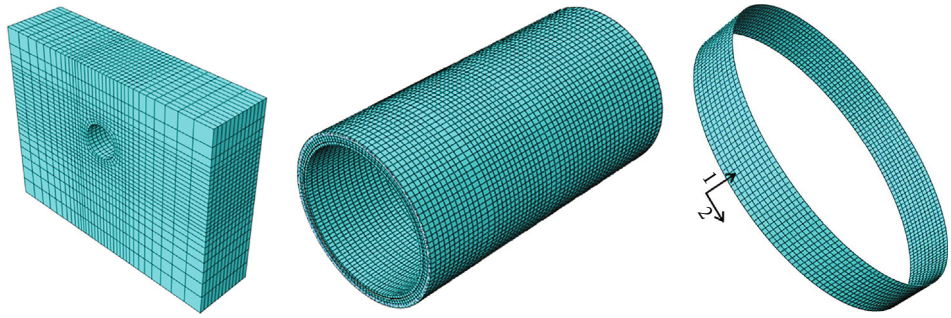

(a) (b) (c)

Figure 3: Three-dimensional mesh: (a) soil; (b) PCCP; (c) CFRP.

Table 2: Material parameters.

Material	Density (kg/m^3)	Elastic modulus (MPa)	Poisson ratio	Tensile strength (MPa)
Concrete	2500	34500	0.2	2.64
Steel cylinder	7850	206000	0.3	215
Prestressing wire	7850	205000	0.3	1570
Mortar	2400	24165	0.2	3.49
CFRP	1796	240000	0.307	3400
PCCP foundation	1890	80	0.29	
Soil cushion	2200	40	0.35	
Backfilling soil	1890	30	0.35	

during the period of operation were analyzed. The stresses and strains of the concrete core, steel cylinder, prestressing wires, and CFRP at different positions were compared.

3.1. Effect of CFRP Repair on the Concrete Core. Figures 5 and 6 show the circumferential strain of the outer and inner concrete cores during the period of operation. In the Figures, the abscissa shows the distance along the length of the PCCP and the ordinate shows the circumferential strain.

The Figures show that the concrete core had maximum strain at the springline of the PCCP and that the springline was the weakest position. Using externally bonded CFRP to repair a PCCP with broken wires significantly reduces the circumferential strain of the concrete core at the springline. Reduced strain on the outer concrete core can be clearly seen, and the concrete strain at the springline showed the greatest reduction when CFRP thickness was 0.334 mm. As the CFRP thickness increased, the effect of the repair increased linearly. However, the strain of the concrete at the crown and the invert changed very little.

In summary, using externally bonded CFRP to repair a PCCP with broken wires significantly increases the stress of the concrete core at the springline, especially for the outer concrete core and less so for the inner concrete core, and there was almost no effect at the crown and the invert. Along the length of the PCCP, the affected area of the concrete was about 3.3 times that of the broken-wire area.

Figure 7 shows the strain maps of the outer concrete core at the springline under the combined loads. It shows the effects of the repair using the externally bonded CFRP. It can be seen that the concrete strain decreased as CFRP thickness increased. The strain in the middle section of the PCCP was larger and gradually decreased towards the ends, which is consistent with Figure 5.

3.2. Effect of CFRP Repair on the Steel Cylinder. Figure 8 shows the circumferential strain of the steel cylinder during the period of operation. The abscissa shows the length of the pipe and the ordinate shows the circumferential strain.

The Figure shows that the strain of the steel cylinder was similar to that of the concrete core. Using externally bonded CFRP to repair a PCCP with broken wires significantly reduces the circumferential strain of the steel cylinder at the springline. The steel cylinder strain at the springline showed the greatest reduction when CFRP thickness was 0.334 mm; as the CFRP thickness further increased, the steel cylinder strain at the springline still decreased. However, the CFRP repair had little effect on the circumferential strain of the steel cylinder at the crown or the invert. The affected area of the steel cylinder along the PCCP was about 3.3 times that of the broken-wire area, which is consistent with the effects on the concrete core.

3.3. Effect of CFRP Repair on the Prestressing Wires. Figure 9 is the strain diagram of the prestressing wires during the period of operation. The abscissa shows the distance along the length of the PCCP, and the ordinate shows the circumferential strain.

The Figure shows that the strain of the prestressing wires at the springline was slightly greater than those at the crown and the invert, similar to the strain of the concrete and the steel cylinder. When the CFRP thickness was 0.334 mm, the strain of the prestressing wires at the springline decreased significantly. However, as the CFRP thickness increased, the strain of the prestressing wires hardly changed. The strain of the prestressing wires at the crown and the invert changed very little as the CFRP thickness changed. The affected area of the prestressing wires was about 3.3 times that of the broken-wire area along the length of the PCCP, which is consistent with the previous analysis.

3.4. Analysis of CFRP Stress. Figure 10 is the circumferential strain diagram of CFRP during the period of operation. The

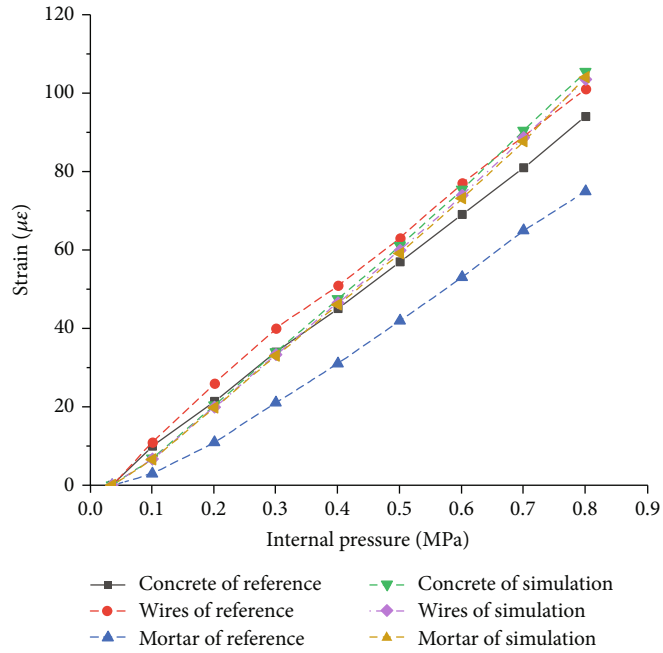

Figure 4: Strain comparisons between PCCP model and reference results.

Table 3: The five models.

Model name[1]	P-t-0	P-t-2	P-t-4	P-t-6	P-t-8
The thickness of CFRP(mm)	Unrepaired	0.334	0.668	1.002	1.336

[1]P is pipe, t is thickness, and the number indicates the number of layers of CFRP at 0.167 mm per layer.

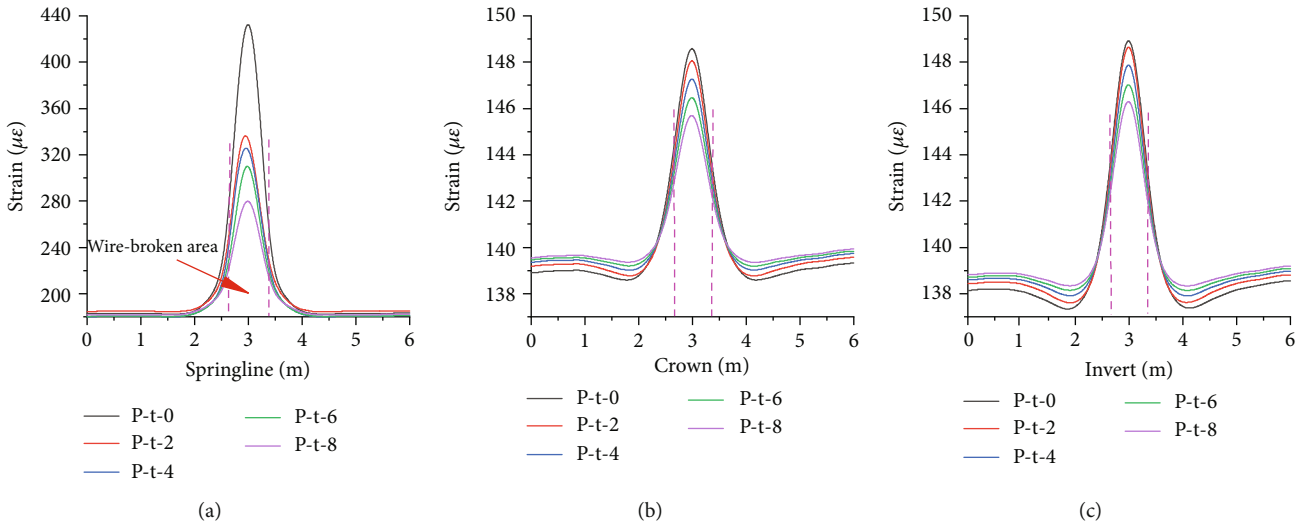

Figure 5: Circumferential strain of the outer concrete core: (a) springline; (b) crown; (c) invert.

abscissa shows the CFRP thickness and the ordinate shows the corresponding strain.

The Figure shows that the CFRP strain at the springline was significantly greater than that at the crown or the invert and that CFRP strain at the springline decreased as the thickness increased. When CFRP thickness reached 0.668 mm, the decreasing trend lessened. The CFRP strains at the crown and the invert were almost unaffected by CFRP thickness, which agrees with the analysis of the results for the concrete core, steel cylinder, and prestressing wires.

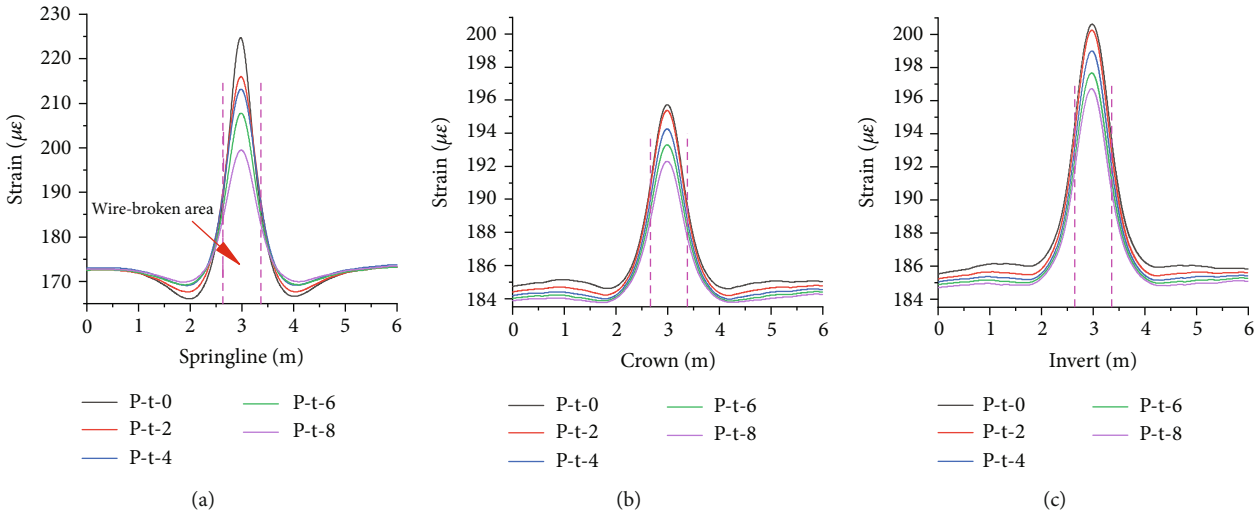

Figure 6: Circumferential strain of the inner concrete core under combined loads: (a) springline; (b) crown; (c) invert.

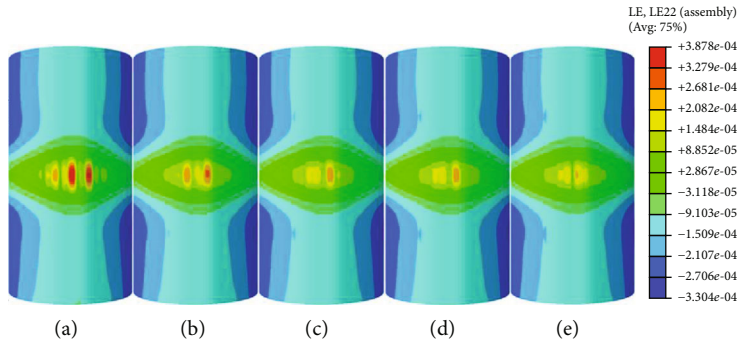

Figure 7: Strain maps of outer concrete core at the springline under combined loads: (a) P-t-0; (b) P-t-2; (c) P-t-4; (d) P-t-6; (e) P-t-8.

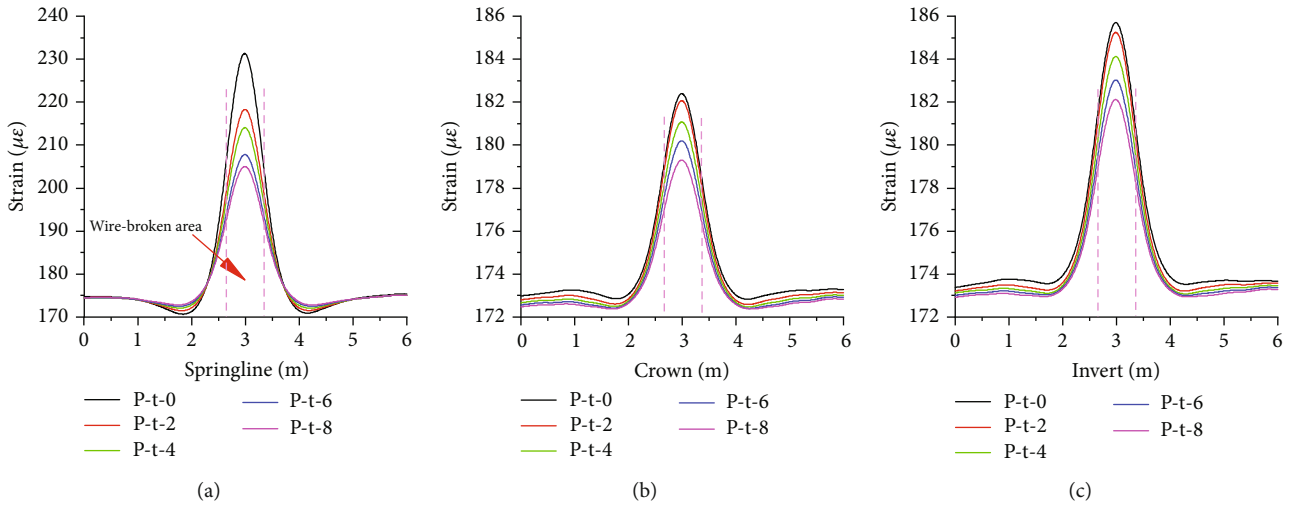

Figure 8: Circumferential strain of the steel cylinder under combined loads: (a) springline; (b) crown; (c) invert.

Figure 11 shows the stress maps of CFRP under combined internal and external loads. The maps show that when the thickness of CFRP was 0.334 mm, CFRP stress was about 136 MPa, which was much less than the ultimate tensile strength. As CFRP thickness increased, the stress gradually decreased.

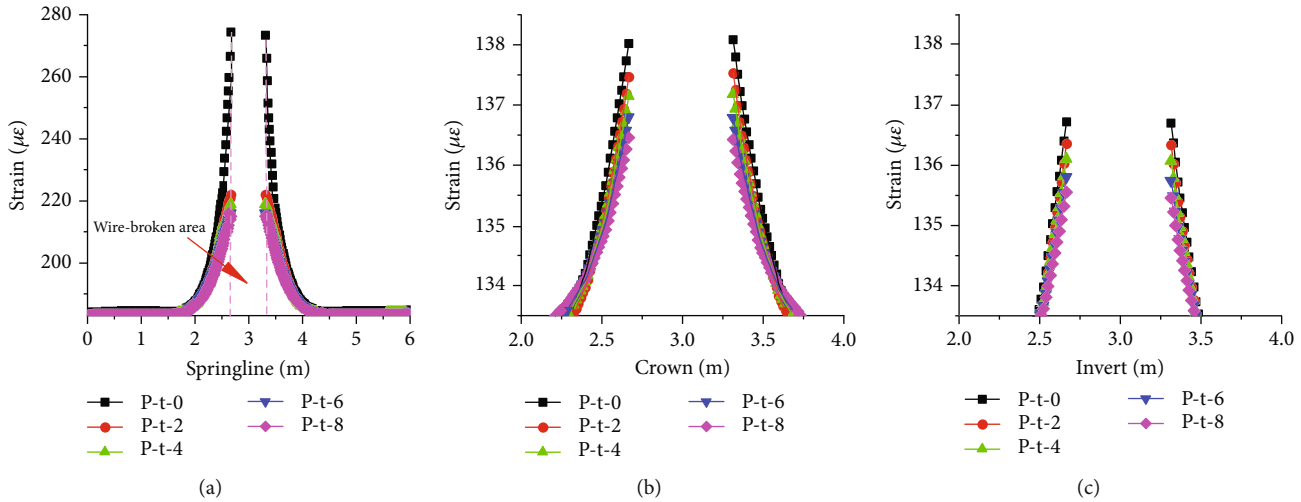

Figure 9: Strain of prestressing wires under combined loads: (a) springline; (b) crown; (c) invert.

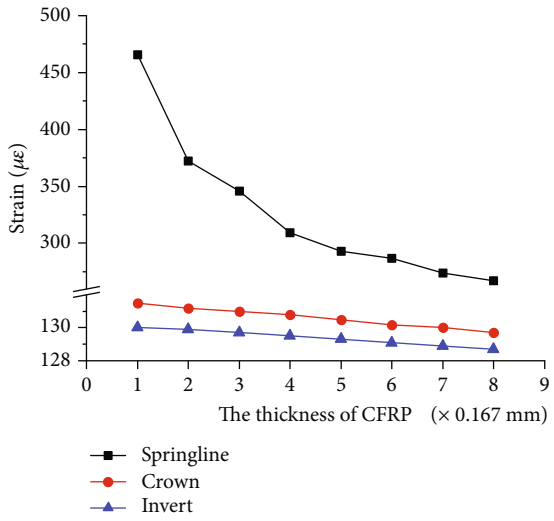

Figure 10: Strain of CFRP under combined loads.

4. Effects of Repairs for Different Wire Breakage Rates

In practice, the number of broken wires may vary for different PCCPs. Therefore, we examined the effects of a repair for different wire breakage rates. The CFRP was 500 mm wide and 1.002 mm thick in the models used for this analysis. The wire breakage rates were 5%, 10%, 15% and 20%. The models are shown in Figure 12.

We examined the effects of the repair on the whole pipe during the period of operation at a hydrostatic pressure of 1.12 MPa, which is the designed value. We compared the stress and strain of the concrete core, steel cylinder, prestressing wires and CFRP when the wire breakage rates were different.

4.1. Effect of Wire Breakage Rates on the Concrete Core. The damage maps of the concrete core under the combined internal pressure and external loads are shown in Figure 13. The Figure shows that when the wire breakage rate was 5%, there was no damage to the concrete core. As the wire breakage rate increased, damage to the concrete core gradually increased. When the wire breakage rate was 10%, a little tensile damage occurred at the middle of the springline. However, the damage was not serious, and there was no damage to the concrete core at the crown or the invert, and the PCCP operates normally. When the wire breakage rate reached 15%, the concrete damage was serious at the springline, and the damage extended to the crown and the invert. At a 20% wire breakage rate, serious damage occurred around the entire circumference at the center of the pipe, but the two ends of the pipe were almost unaffected.

The concrete damage levels suggest that CFRP 500 mm wide and 1.002 mm thick can repair a PCCP having a wire breakage rate of <10%, but when the rate is greater, the method of repair must be reconsidered.

4.2. Effect of Wire Breakage Rates on the Steel Cylinder. Figure 14 shows the circumferential strain of the steel cylinder during the period of operation. The abscissa shows the distance along the length of the PCCP, and the ordinate shows the circumferential strain. The Figure shows that the strain at the springline was greater than at the crown or the invert. When the wire breakage rate was 5%, there was almost no effect on the steel cylinder. As the wire breakage rate increased, the strain of the steel cylinder increased at the center of the pipe. When the wire breakage rate was 20%, the circumferential strain of the steel cylinder was 1025 $\mu\varepsilon$, and the steel cylinder yielded. The wire breakage rate had a significant effect on the steel cylinder.

4.3. Effect of Wire Breakage Rates on the Prestressing Wires. Figure 15 shows the strain of the prestressing wires during the operation period. The abscissa shows the length of the PCCP, and the ordinate shows the strain. The Figure shows that the strain of the prestressing wires at the springline was greater than at the crown or the invert. The strains of the crown and the invert did not change much when the wire

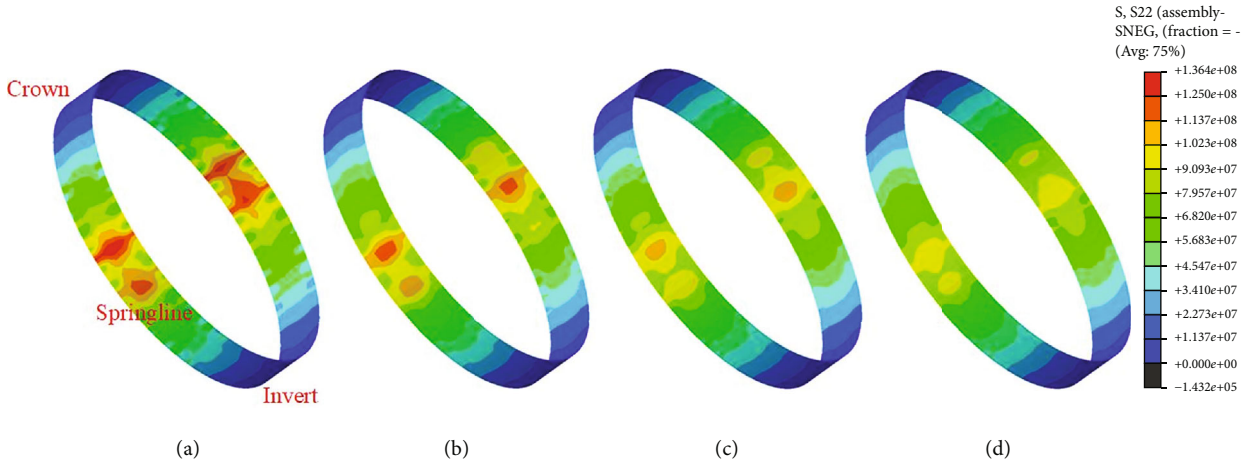

Figure 11: Stress maps of CFRP under combined loads: (a) P-t-2; (b) P-t-4; (c) P-t-6; (d) P-t-8.

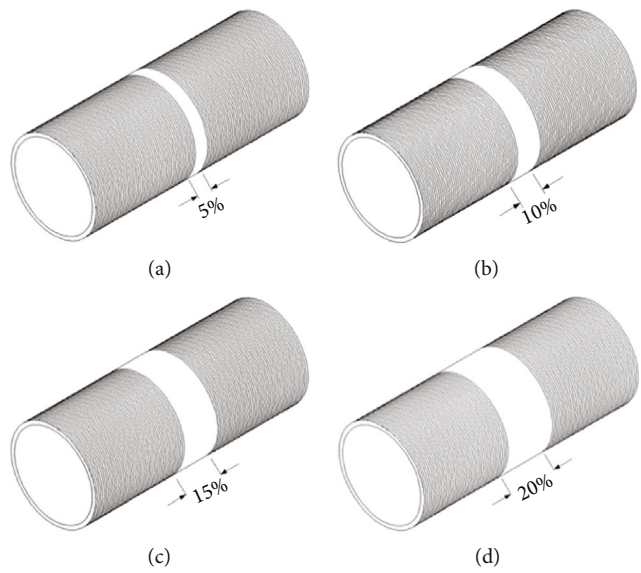

Figure 12: The different models: (a) P-r-5; (b) P-r-10; (c) P-r-15; (d) P-r-20. (P is pipe, r is rate, and the number is the value of the wire breakage rate).

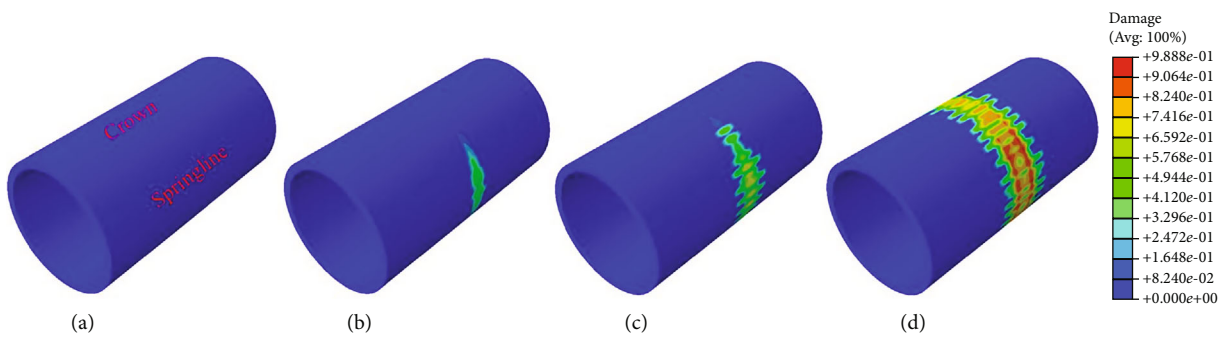

Figure 13: Concrete damage under combined loads: (a) P-r-5; (b) P-r-10; (c) P-r-15; (d) P-r-20.

breakage rate increased from 5% to 10%. In general, the wire breakage rate had a large influence on prestressing wire strain.

4.4. Effect of Wire Breakage Rates on CFRP. Figure 16 shows the circumferential strain of the CFRP during the period of operation. The abscissa shows the wire breakage rates and

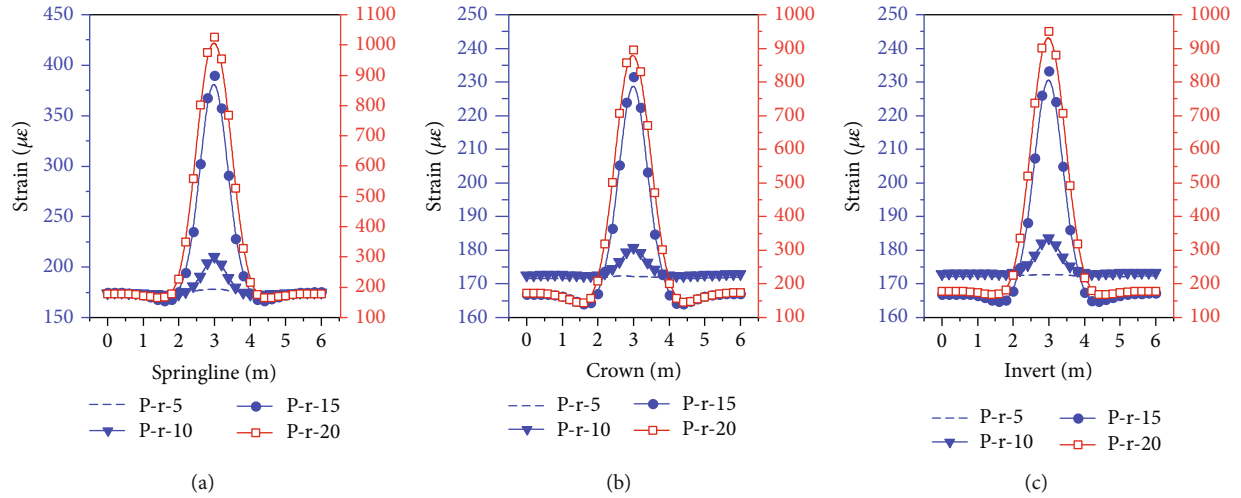

Figure 14: Strain of steel cylinder under combined loads: (a) spring; (b) crown; (c) invert.

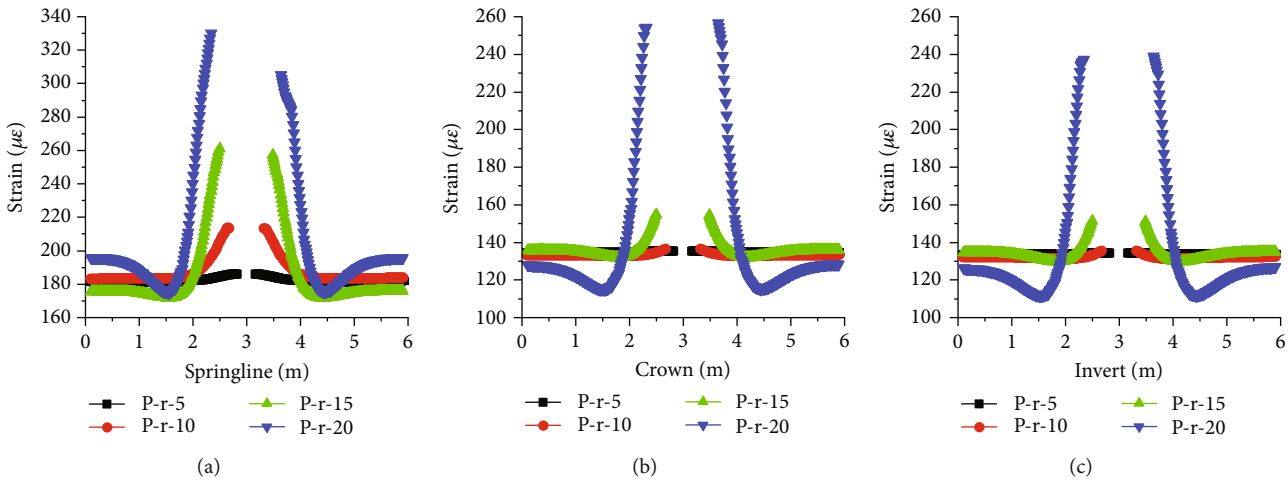

Figure 15: Strain of prestressing wires under combined loads: (a) springline; (b) crown; (c) invert.

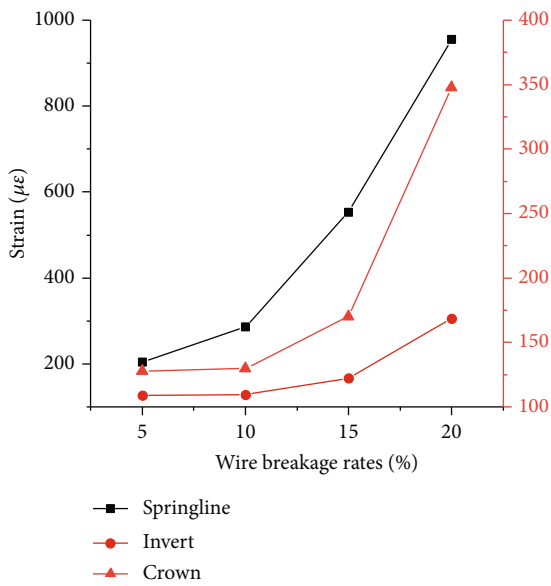

Figure 16: Strain of CFRP under combined loads.

the ordinate shows the circumferential strain. The Figure shows that CFRP strain at the springline was greater than at the crown or the invert. CFRP strains at the crown and at the invert did not change much when the wire breakage rate increased from 5% to 10%. This phenomenon was consistent with the results for the strain of prestressing wires. The wire breakage rates had a significant effect on CFRP. Figure 17 shows the stress maps of CFRP under combined loads. The maximum CFRP stress was 290.6 MPa when the wire breakage rate was 20%, which was much less than the ultimate tensile strength.

5. Conclusion

In this study, externally bonded CFRP of different thicknesses was used to repair a PCCP with broken wires. We constructed a three-dimensional finite element model of the repaired PCCP, using ABAQUS software, that took into account the pressure of the soil, the weight of the water, the weight of the PCCP, and the hydrostatic pressure. The effects of the repairs on each PCCP component material for

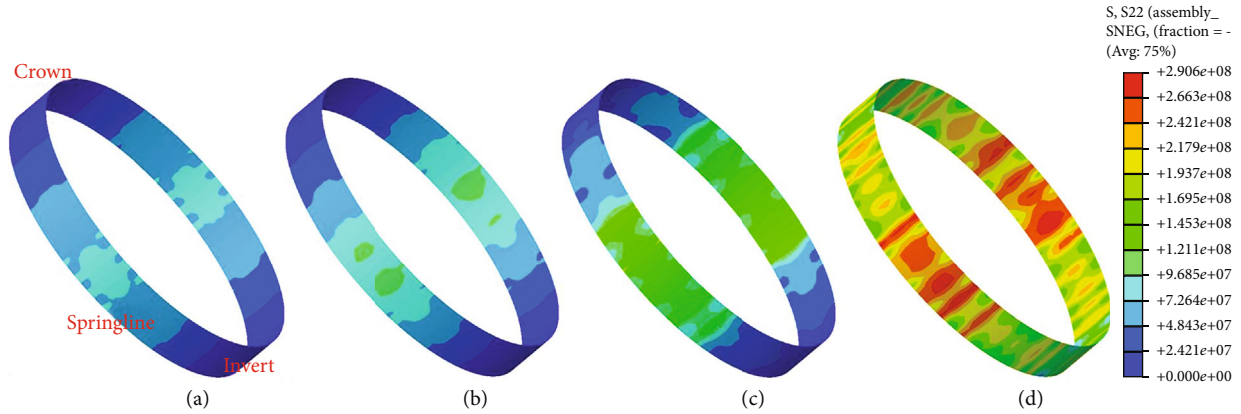

Figure 17: Stress maps of CFRP under combined loads: (a) P-r-5; (b) P-r-10; (c) P-r-15; (d) P-r-20.

different CFRP thicknesses and different wire breakage rates were analyzed. The main conclusions are as follows.

(1) Under the combined loads, the stresses of the concrete core and the prestressing wires were greater at the springline than at the crown or the invert. The strain at the springline can be reduced by repairing the PCCP with the CFRP.

(2) When the rate of wire breakage was 10%, the strained area of each material was about 3.3 times the broken-wire area along the length of the PCCP; when the rate of wire breakage was <10%, CFRP that is 1.002 mm thick and 500 mm wide can be used for repair.

(3) The rate of wire breakage had a large influence on the strain of each material. However, the stress of CFRP is much less than its tensile strength.

Data Availability

The data used to support the findings of this study are available from the corresponding author upon request.

Conflicts of Interest

The authors declare that they have no conflicts of interest.

Acknowledgments

This work was supported by the National Key Research and Development Program of China (No. 2016YFC0802400), the National Natural Science Foundation of China (No. 51978630, 51678536), the Program for Science and Technology Innovation Talents in Universities of Henan Province (Grant No. 19HASTIT043), the Outstanding Young Talent Research Fund of Zhengzhou University (1621323001) and the Program for Innovative Research Team (in Science and Technology) in University of Henan Province (18IRTSTHN007). The authors would like to thank for these financial supports.

References

[1] ANSI/AWWA C304-2014, *Design of Prestressed Concrete Cylinder Pipe*, American National Standards Institute, American Water Works Association, 2014.

[2] SL702-2015, *Technical Specifications of Prestressed Concrete Cylinder Pipe*, Beijing: China Water & Power Press, 2015.

[3] C. W. Ross, "Tests of prestressed concrete pipes containing a steel cylinder," *ACI Journal Proceedings*, vol. 42, no. 9, pp. 37–48, 1945.

[4] H. F. Kennison, "Tests on prestressed concrete embedded cylinder pipe," *Journal of the Hydraulics Division*, vol. 86, no. 9, pp. 77–98, 1960.

[5] J. T. Mccall and F. P. Valenziano, "Combined load tests on 108 inch prestressed concrete embedded cylinder pipe," in *Proceedings of Symposia on Prestressed Concrete*, pp. 1–16, Sidney, Australia, 1961.

[6] R. Gomez, D. Muñoz, R. Vera, and J. A. Escobar, "Structural model for stress evaluation of Prestressed concrete pipes of the Cutzamala system," *Pipeline Engineering*, vol. 21, pp. 831–856, 2004.

[7] S. R. Zhang and C. X. Zhang, "Numerical simulation analysis of prestressed concrete cylinder pipe," *Journal of Harbin Institute of Technology*, vol. 41, no. 8, pp. 118–122, 2009.

[8] T. S. Dou, B. Q. Cheng, H. Hu, S. F. Xia, J. X. Yang, and Q. Zhang, "The prototype test study of prestressed concrete cylinder pipe structure deformation law I. the internal pressure," *Journal of Hydraulic Engineering*, vol. 48, no. 12, pp. 1438–1446, 2017.

[9] T. S. Dou, B. Q. Cheng, H. Hu, S. F. Xia, J. X. Yang, and Q. Zhang, "The prototype test study of prestressed concrete cylinder pipe structure deformation law II. The external pressure," *Journal of Hydraulic Engineering*, vol. 49, no. 2, pp. 207–215, 2018.

[10] Y. Zhang, Z. G. Yan, H. H. Zhu, and J. W. Ju, "Experimental study on the structural behaviors of jacking prestressed concrete cylinder pipe," *Tunnelling and Underground Space Technology*, vol. 73, pp. 60–70, 2018.

[11] M. S. Zarghamee, R. P. Ojdrovic, and W. R. Dana, "Coating delamination by radial tension in Prestressed concrete pipe. I: experiments," *Journal of Structural Engineering*, vol. 119, no. 9, pp. 2701–2719, 1993.

[12] M. S. Zarghamee, R. P. Ojdrovic, and W. R. Dana, "Coating delamination by radial tension in Prestressed concrete pipe.

II: analysis," *Journal of Structural Engineering*, vol. 119, no. 9, pp. 2720–2732, 1993.

[13] S. W. Hu, J. Shen, D. L. Wang, and X. Cai, "Experiment and numerical analysis on super caliber prestressed concrete cylinder pipes with cracks," *Journal of Hydraulic Engineering*, vol. 41, no. 7, pp. 876–882, 2010.

[14] Q. Gong, H. Zhu, Z. Yan, B. Huang, Y. Zhang, and Z. Dong, "Fracture and delamination assessment of prestressed composite concrete for use with pipe jacking method," *Mathematical Problems in Engineering*, vol. 2015, Article ID 579869, 11 pages, 2015.

[15] L. Q. Sun, J. J. Zhang, H. Li, S. W. Yan, and Z. L. Huo, "Research on key factors influencing relative angle of prestressed concrete cylinder pipe in soft soil foundation," *Rock and Soil Mechanics*, vol. 36, no. S1, pp. 293–298, 2015.

[16] Y. Zhang, Z. G. Yan, and H. H. Zhu, "Site-based researches on mechanical behavior of new large-diameter pipes during pipe jacking," *Chinese Journal of Geotechnical Engineering*, vol. 39, no. 10, pp. 1842–1850, 2017.

[17] Z. Xu, X. Feng, S. Zhong, and W. Wu, "Surface crack detection in Prestressed concrete cylinder pipes using BOTDA strain sensors," *Mathematical Problems in Engineering*, vol. 2017, Article ID 9259062, 12 pages, 2017.

[18] Y. G. Diab and T. Bonierbale, "A numerical modeling and a proposal for rehabilitation of PCCPs," in *Pipeline Division Specialty Conference 2001*, pp. 1–8, San Diego, California, United States, 2001.

[19] M. S. Zarghamee, D. W. Eggers, and R. P. Ojdrovic, "Finite-element modeling of failure of PCCP with broken wires subjected to combined loads," in *Pipeline Division Specialty Conference 2002*, pp. 1–17, Cleveland, Ohio, United States, 2002.

[20] M. S. Zarghamee, "Hydrostatic pressure testing of prestressed concrete cylinder pipe with broken wires," in *Pipeline Engineering and Construction International Conference 2003*, pp. 294–303, Baltimore, Maryland, United States, 2003.

[21] M. S. Zarghamee, D. W. Eggers, R. P. Ojdrovic, and B. Rose, "Risk analysis of Prestressed cylinder pipe with broken wires," *Pipelines*, vol. 83, pp. 599–609, 2003.

[22] S. W. Hu and J. Shen, "Study on impact from wire-breaking inside of super-large diameter PCCP on its bearing capacity," *Water Resources and Hydropower Engineering*, vol. 42, no. 4, pp. 41–44, 2011.

[23] S. Ge and S. Sinha, "Effect of mortar Coating's bond quality on the structural integrity of Prestressed concrete cylinder pipe with broken wires," *Journal of Materials Science Research*, vol. 4, no. 3, pp. 59–75, 2015.

[24] M. Hajali, A. Alavinasab, and C. A. Shdid, "Effect of the location of broken wire wraps on the failure pressure of prestressed concrete cylinder pipes," *Structural Concrete*, vol. 16, no. 2, pp. 297–303, 2015.

[25] M. Hajali, A. Alavinasab, and C. A. Shdid, "Effect of the number of broken wire wraps on the structural performance of PCCP with full interaction at the gasket joint," *Journal of Pipeline Systems Engineering and Practice*, vol. 7, no. 2, article 04015026, 2016.

[26] M. Hajali, A. Alavinasab, and C. Abi Shdid, "Structural performance of buried prestressed concrete cylinder pipes with harnessed joints interaction using numerical modeling," *Tunnelling and Underground Space Technology*, vol. 51, pp. 11–19, 2016.

[27] J.-Y. Lee, H.-O. Shin, K.-H. Min, and Y.-S. Yoon, "Flexural assessment of blast-damaged rc beams retrofitted with cfrp sheet and steel fiber," *International Journal of Polymer Science*, vol. 2018, Article ID 2036436, 9 pages, 2018.

[28] G. Cicala, G. Cristaldi, G. Recca, G. Ziegmann, A. Elsabbagh, and M. Dickert, *An Hybrid Glass/Hemp Fibers Solution FRP Pipes: Technical and Economic Advantages of Hand Lay up Vs Light RTM*, American Institute of Physics, 2008.

[29] G. Cicala, G. Cristaldi, G. Recca, G. Ziegmann, A. el-Sabbagh, and M. Dickert, "Properties and performances of various hybrid glass/natural fibre composites for curved pipes," *Materials & Design*, vol. 30, no. 7, pp. 2538–2542, 2009.

[30] G. Cicala, I. Blanco, A. Latteri, G. Ognibene, F. Agatino Bottino, and M. Fragalà, "PES/POSS soluble veils as advanced modifiers for multifunctional Fiber reinforced composites," *Polymers*, vol. 9, no. 12, p. 281, 2017.

[31] D. C. Lee and V. M. Karbhari, "Rehabilitation of large diameter Prestressed cylinder concrete pipe (PCCP) with FRP composites–experimental investigation," *Advances in Structural Engineering*, vol. 8, no. 1, pp. 31–44, 2005.

[32] M. Engindeniz, R. P. Ojdrovic, and M. S. Zarghamee, "Quality assurance procedures for repair of concrete pressure pipes with CFRP composites," in *Pipelines Conference 2011*, pp. 616–627, Seattle, Washington, United States, 2011.

[33] M. Engindeniz and M. S. Zarghamee, "Experimental basis of CFRP renewal of PCCP," in *Pipelines 2014*, pp. 920–931, Portland, Oregon, 2014.

[34] T. Alkhrdaji, S. Rocca, and N. Galati, "PCCP rehabilitation using advanced hybrid FRP composite liner," in *Pipelines 2013*, pp. 672–681, Fort Worth, Texas, United States, 2013.

[35] Y. Lee and E. T. Lee, "Analysis of prestressed concrete cylinder pipes with fiber reinforced polymer," *KSCE Journal of Civil Engineering*, vol. 19, no. 3, pp. 682–688, 2015.

[36] H. Hu, F. Niu, T. Dou, and H. Zhang, "Rehabilitation effect evaluation of CFRP-lined Prestressed concrete cylinder pipe under combined loads using numerical simulation," *Mathematical Problems in Engineering*, vol. 2018, Article ID 3268962, 16 pages, 2018.

[37] B. Li, H. Y. Fang, H. He, K. J. Yang, C. Chen, and F. M. Wang, "Numerical simulation and full-scale test on dynamic response of corroded concrete pipelines under multi-field coupling," *Construction and Building Materials*, vol. 200, pp. 368–386, 2019.

[38] H. Xiong, P. Li, and Q. Li, "FE model for simulating wire-wrapping during prestressing of an embedded prestressed concrete cylinder pipe," *Simulation Modelling Practice and Theory*, vol. 18, no. 5, pp. 624–636, 2010.

[39] H. Fang, B. Li, F. Wang, Y. Wang, and C. Cui, "The mechanical behaviour of drainage pipeline under traffic load before and after polymer grouting trenchless repairing," *Tunnelling and Underground Space Technology*, vol. 74, pp. 185–194, 2018.

[40] F. M. Wang, H. Y. Fang, B. Li, and C. Chen, "Dynamic response analysis of drainage pipe with gasketed bell-and-spigot joints subjected to traffic load," *Chinese Journal of Geotechnical Engineering*, vol. 40, no. 12, pp. 2274–2280, 2018.

[41] B. Hu, H. Fang, F. Wang, and K. Zhai, "Full-scale test and numerical simulation study on load-carrying capacity of prestressed concrete cylinder pipe (PCCP) with broken wires under internal water pressure," *Engineering Failure Analysis*, vol. 104, pp. 513–530, 2019.